https://doi.org/10.5194/egusphere-2026-2789
Preprint. Discussion started: 5 June 2026

Morphological and phylogenic variability of red snow algae in snow-packs along a glacial valley in Alaska

Masato Ono[1, 2, 3*], Kino Kobayashi[1], Takumi Suzuki[1,4], Ryohei Abe[1], Suzunosuke Usuba[1], Jun Uetake[5] and Nozomu Takeuchi[6]

[1]Graduate School of Science and Engineering, Chiba University, Chiba, Japan
[2]Center for Ecological Research, Kyoto University, Shiga, Japan
[3]Graduate School of Arts and Sciences, The University of Tokyo,Tokyo, Japan
[4]Earth Observation Research Center, Japan Aerospace Exploration Agency, Ibaraki, Japan
[5]Field Science Center for Northern Biosphere, Hokkaido University, Hokkaido, Japan
[6]Center for Environmental Remote Sensing, Chiba University, Chiba, Japan

Correspondence to: Masato Ono (masatono@g.ecc.u-tokyo.ac.jp)

Abstract. Red snow blooms are visually similar but can be composed of different algal species and cell morphologies across sites, and the factors determining this spatial heterogeneity remain poorly understood. In this study, we investigated spatial variation in community structure, algal cell size, and morphology along gradients of elevation across a glacier and its forefield in Alaska. Microscopic observations revealed that the ice-based snowpack was dominated by spherical cells, whereas the soil-based snowpack was characterized by a higher abundance of non-spherical cells and larger spherical cells. Molecular analyses revealed that *Sanguina* predominated in the ice-based snowpack, while the relative abundance of other genera, including *Chloromonas* and *Rosetta*, were more abundant in the soil-based snowpack. Redundancy analysis showed that community structure was explained primarily by snow depth and elevation, whereas it was not significantly influenced by nutrient concentrations. Generalized linear models further indicated that size of spherical cell decreased with elevation, and the proportion of non-spherical cells decreased with snow depth. These results suggest that while snowmelt-driven environmental gradients govern the overall morphological and phylogenetic variability of red snow algae, the underlying substrate (ice vs. soil) also contributes to community turnover, likely by providing access to distinct local cell reservoirs during melt progression. Collectively, these factors shape the taxonomic composition, morphotype assemblage, and spatial development of red snow blooms.

1 Introduction

Snow algae are photosynthetic microorganisms adapted to cold environments that actively grow in snowpacks during the snowmelt season. In polar and alpine snowpacks, environmental stress (e.g., intense ultraviolet radiation, low temperatures, freeze-thaw cycles, and nutrient limitation) induces the accumulation of secondary carotenoid pigments, causing red snow (Remias *et al.* 2005; Leya *et al.* 2009; Hoham & Remias 2020). Red snow markedly reduces surface albedo and accelerates

https://doi.org/10.5194/egusphere-2026-2789
Preprint. Discussion started: 5 June 2026

snowmelt (Yallop *et al.* 2012; Cook *et al.* 2017), highlighting biologically mediated albedo (bioalbedo) feedback on the energy balance at the snow surface (Lutz *et al.* 2016; Hotaling *et al.* 2021; Roussel *et al.* 2024).

Research on red snow algae has primarily focused on their phylogenetic classification. Red snow is mainly caused by algae belonging to the genera *Sanguina* (Procházková *et al.* 2019), *Chloromonas* (Novakovskaya *et al.* 2018; Procházková *et al.* 2024), *Rosetta* (Engstrom *et al.* 2024), and *Chlainomonas* (Novis 2002; Procházková *et al.* 2018). Among these, *Sanguina nivaloides* (originally classified as *Chlamydomonas nivalis*; Procházková *et al.* 2019) is characterized by spherical cells and is widely distributed in snowpacks globally (Segawa *et al.* 2018). In contrast, other genera exhibit a wide diversity of morphotypes (Novakovskaya *et al.* 2018; Engstrom *et al.* 2024; Procházková *et al.* 2024), and their occurrence appears to be more spatially heterogeneous, often showing regionally distinct morphotypes and community structure (Nakashima *et al.* 2021; Almela *et al.* 2025).

Morphotypes of snow algae exhibit substantial diversity depending on life cycle stage even within a single species. Many red snow forming taxa exhibit marked morphological transitions from small flagellated or vegetative cells to enlarged non motile resting cells associated with carotenoid accumulation during late developmental stages (Procházková *et al.* 2019; Hoham & Remias 2020). At the same time, morphologically distinct forms can occur among different taxa, whereas some unrelated taxa may display similar morphotypes, making species level identification based solely on morphology difficult (Novakovskaya *et al.* 2018; Engstrom *et al.* 2024). In particular, spherical cells, commonly observed in red snow, show substantial variation in cell size across sites and life cycle stages. This size variability may reflect differences in community structure, but it may also arise within a single species in response to environmental conditions or developmental stage (Procházková *et al.* 2019; Hoham & Remias 2020). Consequently, morphological traits alone do not necessarily correspond directly to taxonomic identity and may instead reflect physiological status or life cycle progression. Because physically based bioalbedo models represent algal cells as light-absorbing particles with explicit geometric dimensions, variation in cell size is potentially relevant not only to taxonomy and physiology but also to snow optical properties and albedo reduction (Cook *et al.* 2017). However, the primary factors determining resulting morphotype and community structure in snowpacks remain poorly understood.

Within the same region, spatial variation in algal community structure has often been discussed in relation to differences in algal life cycles, especially in their sources that supply cells to the snow surface. These sources can be broadly divided into two pathways: atmospheric deposition and supply from the subsurface. Some species (e.g., *Sanguina nivaloides* and *Chloromonas nivalis*), are delivered to snowpacks through atmospheric transport and deposition, including wind and snowfall, which can disperse algae over long distances (Muller *et al.* 1998; Hoham & Duval 2001). Other species, including locally retained forms such as resting cysts of *Sanguina nivaloides* and vegetative or cyst stages of *Chlainomonas rubra*, can originate from local reservoirs, such as cysts retained within the snowpack or cells associated with underlying firn, ice surface, soils, and vegetation. An experimental field study on the Harding Icefield demonstrated that algal blooms can be dominated by resurfacing cysts of *Sanguina nivaloides* originating from subsurface snow and firn overlying glacier ice, rather than being solely supplied by passive deposition (Rea and Dial 2024). Field observations and life cycle syntheses further support that cells such as *Sanguina nivaloides* from deeper snow layers over glacier ice and *Chlainomonas rubra* originating from snow–ground or

https://doi.org/10.5194/egusphere-2026-2789
Preprint. Discussion started: 5 June 2026

soil interfaces can become available at the snow surface as meltwater connects pore spaces and layers during the melt season (Hoham and Duval 2001; Matsumoto et al. 2024). Within this framework, snowmelt duration can be viewed as an approximation of the time available for in situ algal growth, while snow depth can constrain how readily locally sourced cells reach the snow surface. However, direct comparisons between contrasting underlying environments such as glacier ice and soil within the same region have not been conducted to evaluate this framework.

Various studies on red snow algae have been conducted in Alaska, making it an ideal region to evaluate these ideas. In addition to its extensive glaciated landscapes, North America, including Alaska and Arctic Canada, is known to host a particularly high diversity of snow algal taxa and morphotypes, with multiple co-occurring lineages such as *Sanguina*, *Chloromonas*, and the recently described Rosetta group showing regionally distinct community compositions (Kol 1968; Novakovskaya *et al.* 2018; Procházková *et al.* 2019; Engstrom *et al.* 2024). This diversity suggests that spatial variation in community structure is likely to be especially pronounced in this region, providing an opportunity to examine how environmental gradients shape algal assemblages. Satellite-based work on the Harding Icefield further demonstrated that red snow distribution can be mapped at landscape scales, indicating a broad spatial structure in algal bloom (Takeuchi *et al.* 2006). At the cellular level, detailed microscopy and spectroscopy have revealed multiple morphotypes with distinct fluorescence and pigment-related characteristics, indicating functional diversity even within visually similar blooms (Fiołka *et al.* 2020). Despite these advances, existing studies have rarely integrated glaciers and forefield snowpacks within a single glacial valley framework, nor have they systematically compared surface and subsurface snow layers, to explain how community structure and morphological traits co-occur in red snow.

This study aimed to characterize the spatial variability of community structure and morphological traits in snowpacks along a glacial valley in Alaska, where snow algae have been previously reported (Takeuchi 2001, 2013; Fiołka *et al.* 2020). We collected red snow from ice-based snowpack and soil-based snowpack during the early melting season. We quantified algal morphotypes and algal community structure using microscopy and molecular approaches and discussed how elevation, snow depth, nutrient availability, and the environment beneath the snow relate to coordinated transitions in community structure and morphotype assemblage.

2 Material and Methods

2.1 Study site and sample collection

The study was conducted in a glacial valley of the Gulkana Glacier in the Alaska Range, USA (Fig. 1a). Gulkana Glacier, located at the valley head, flows southward from the mountain ridge and peaks of 2000 m to 3000 m. The area of the glacier is estimated to be 16.0 km^2 (O'Neel *et al.* 2019). Gulkana Glacier has been a benchmark glacier for long-term observations by the USGS, and meteorological conditions and glacier mass balance have been monitored since the 1960s (U.S. Geological Survey Benchmark Glacier Program *et al.* 2024). The glacier flows down to approximately 1160 m at the current terminus, and the glacial forefield extends downstream. The surface of the forefield was mainly deposits of gravels and silts without

https://doi.org/10.5194/egusphere-2026-2789
Preprint. Discussion started: 5 June 2026

vegetation within approximate 1 km from the glacial terminus, and grass and shrubs appear at 1 km from the glacial terminus (Fig. 1a, b).

Red snow samples were collected at the 30 sites on the snowpack along the valley from July 2nd to 5th, 2023. At the time of sampling, the glacier surface was entirely covered by seasonal snow, and the snowline had not yet retreated above the glacier terminus. In the glacier forefield, the snow cover was patchy and discontinuous. The sampling sites were located on soil-based snowpack (10 sites) and ice-based snowpack (20 sites). In this study, the site farthest downstream from the glacier terminus was defined as S1 (distance from the glacier terminus: 3.6 km), and the remaining sites were numbered consecutively upstream. The boundary between soil-based snowpack and ice-based snowpack was located between S10 and S11. Elevation and snow depth varied systematically along the site sequence, with measured snow depth ranging from 4 to 235 cm across the sampling sites (Fig. 1c). Using a stainless-steel scoop, red snow patches (10 × 10 × 2 cm) were collected, then stored in Whirl-Pak bags. On the ice-based snowpack, red snow patches 3–5 cm in snow depth (10 × 10 × 3 cm) were also collected (Fig. 2). Collected samples were melted and transferred into 6 ml tubes for microscopic observation and chemical analysis. Samples for microscopic observations were stored with 3% formaldehyde. 5 mL of the meltwater was used for the analysis of chemical solutes after filtering through a 0.45 μm ion-free disposable filter to remove microbes and particulate dust. In addition, samples were also transferred into 6 ml tubes for molecular analysis at selected sites located (S1, S4, S7, S9, S10, S14, S22, S25, and S30). Samples for chemical and molecular analyses were transported frozen and stored in a freezer (−20 °C) at Chiba University until analysis whereas samples for microscopic observations were stored at room temperature.

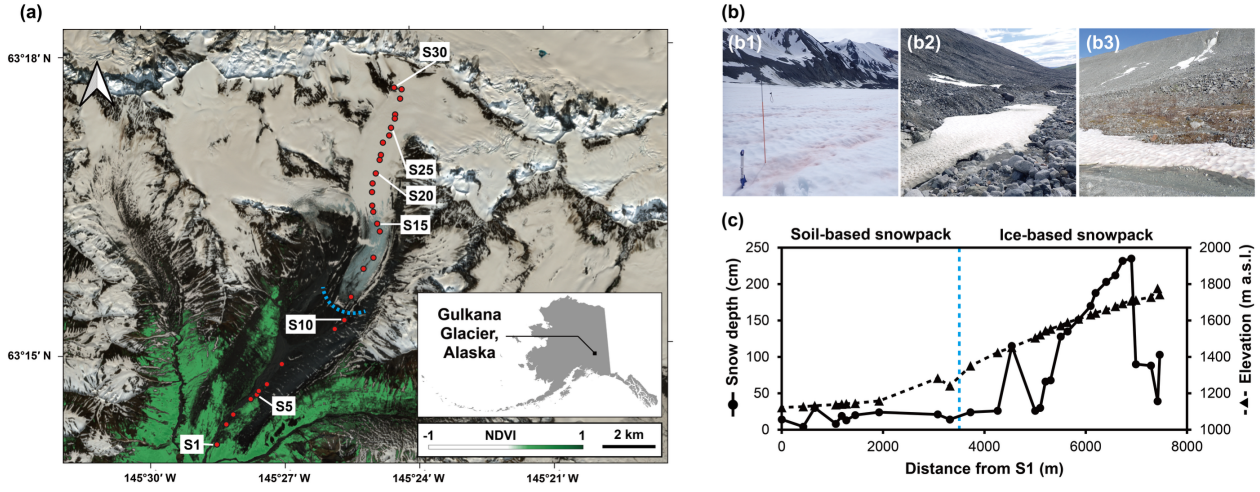

Figure 1: The study site. (a) A map of Gulkana Glacier, red circles indicate locations where samples were collected. The source of a satellite image was captured on June 22nd 2024 by Sentinel-2, and was downloaded from Copernicus browser (https://browser.dataspace.copernicus.eu/, accessed: October 21st 2024). Areas shown in green represent the normalized difference vegetation index (NDVI) calculated by image processing using Image J software. (b) Conditions at the study site: (b1) on-glacier snowpack, (b2) glacier terminus, and (b3) glacier forefield. (c) Snow depth and elevation across the study area. S0 indicates the site farthest from the glacier. The blue dashed line in (a) and (c) indicates the boundary between the glacier and the glacier forefield. In the glacier forefield, although snow cover appears absent at the macro-scale, red snow samples were collected from localized, patchy snow remnants that persisted in topographic depressions as shown in (b2) and (b3).

https://doi.org/10.5194/egusphere-2026-2789
Preprint. Discussion started: 5 June 2026

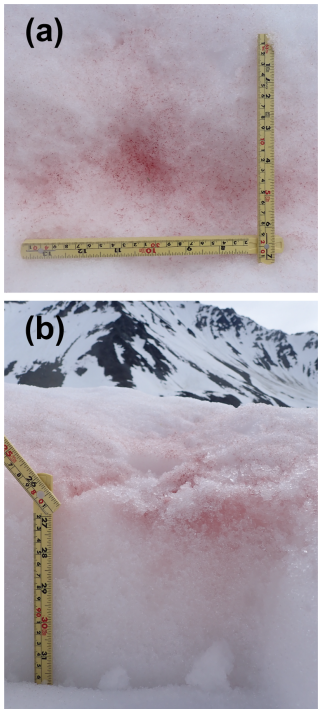

Figure 2: Snowpack conditions. (a) Snow surface. (b) Cross-section of the snowpack.

2.2 Microscopic observations

Microscopic observations were conducted to describe the morphology of the snow algal cells in the samples. The sample (20 µL) was transferred to a slide glass. Images of algae were captured using a fluorescence microscope (BX51, Olympus, Japan) equipped with a digital camera (DP21, Olympus, Japan). The geometric size of the algal cells (diameter or length and width) was measured using an image processing software (ImageJ 1.38X, National Institutes of Health, USA). Additionally, the diameter of spherical cells was measured in a minimum of 100 cells in each sample to describe the distribution of algal cell sizes.

The cell numbers of snow algae in the snow samples were counted to calculate cell concentrations. 100–500 µL aliquots of the sample were collected on a 0.45 µm PTFE membrane filter (JHWP01300, Merck Millipore, Germany), then filtered using a pump (Linicon LV-125, Nitto Kohki, Japan). The filter was then placed on a slide, covered with a cover glass, and immersed in Milli-Q water. Cell counts were performed three times for each sample using a fluorescence microscope. The average cell number and the sample volume used for filtration were used to calculate the cell concentration per water equivalent of the snow sample (cells mL^{-1}). For the samples analyzed by molecular methods, morphotype composition was quantitatively compared with molecular taxonomic composition by calculating volumetric biomass for each morphotype. Total algal biomass was estimated as the sum of the products of algal cell concentration and mean cell volume for each morphotype.

https://doi.org/10.5194/egusphere-2026-2789
Preprint. Discussion started: 5 June 2026

2.3 Chemical analysis

The concentrations of soluble nutrients (NH_4^+, NO_3^- and PO_4^{3-}), were analyzed with an ion-chromatography system (for anion: AQUION, Thermo Fisher Scientific, USA, for cation: ICS-1100, Thermo Fisher Scientific, USA). Concentrations were given in equivalent units per meltwater of snow ($\mu Eq\ Kg^{-1}$).

2.4 DNA sequencing

Genomic DNA of snow samples were extracted using the DNeasy PowerSoil Pro Kit (QIAGEN, Germany) following the manufacturer's protocol. Partial 18S rRNA gene sequences including the V4–V5 regions were amplified using the primers Bakt_341F (CCTACGGGNGGCWGCAG) and 528F (5′-GCGGTAATTCCAGCTCCAA-3′) and 706R (5′-AATCCRAGAATTTCACCTCT-3′) (Cheung *et al.* 2010), with Illumina overhang adapter sequences (Forward: 5′-TCGTCGGCAGCGTCAGATGTGTATAAGAGACAG-3′; Reverse: 5′-GTCTCGTGGGCTCGGAGATGTGTATAA-GAGACAG-3′) attached to their 5′ ends. The PCR reaction mixture was prepared containing 5 U μL^{-1} AmpliTaq Gold DNA Polymerase (Thermo Fisher Scientific, USA), 10× AmpliTaq Gold Buffer (Thermo Fisher Scientific, USA), 10 mM dNTPs, 25 mM $MgCl_2$, and 20 μM of each primer. Polymerase chain reaction (PCR) cycle was performed with an initial denaturation at 94°C for 3 min, followed by 35 cycles of denaturation at 94°C for 15 s, annealing at 54°C for 15 s, and extension at 72°C for 30 s, with a final extension at 72°C for 10 min by CFX96 Touch (Bio-Rad Laboratories, CA, USA). The resulting PCR products were purified using AMPure XP beads (Beckman Coulter, USA). Subsequently, sequencing adapters and index sequences were attached via a second PCR (95°C for 5 min; 10 cycles of 95°C for 30 s, 60°C for 30 s, and 72°C for 30 s; and a final extension at 72°C for 5 min), followed by another purification step with AMPure XP. DNA concentrations were measured using a Quantus™ Fluorometer (Promega Corporation, WI, USA), and all samples were pooled and adjusted to a final DNA amount of 40 ng. Sequencing was performed on a MiSeq using the the MiSeq Reagent Kit v3 (Illumina, USA) at Macrogen Japan.

2.5 Amplicon sequence variant analysis

To understand the community structure of snow algae based on the V4–V5 region sequences, the sequences were classified into amplicon sequence variants (ASVs). Raw reads were processed using the R package "DADA2" (Callahan *et al.* 2016). Quality filtering, trimming, and denoising were performed, including error rate learning and correction. Paired-end reads were merged, and chimeric sequences were removed. Taxonomic assignment was performed using the assign Taxonomy function in DADA2 (Wang *et al.* 2007) against customed Silva 132 database (Callahan 2018). Custom Silva 132 database is including both standard sequences and additional sequences from (Engstrom *et al.* 2024) which studied snow algae genus *Rosetta*, in order to reflect recent taxonomic update. Downstream analyses were conducted using the R packages "microViz" (Barnett *et al.* 2021) and "phyloseq" (McMurdie & Holmes 2013). To determine the proportions of snow algae relative to all eukaryotes

https://doi.org/10.5194/egusphere-2026-2789
Preprint. Discussion started: 5 June 2026

and red snow algae relative to all *Chlorophyta*, relative abundances were calculated for each taxonomic group based on the total number of reads at the phylum or genus level.

2.6 Statistical analysis

Differences in algal abundance, algal cell size, and nutrient concentration were evaluated using Dunn's test. Specifically, comparisons were made between (i) the ice-based snowpack (snow surface) and soil-based snowpack (snow surface), and (ii) the ice-based snowpack (snow surface) and ice-based snowpack (snow subsurface). Generalized linear models (GLMs) were used to examine the relationships between environmental variables and algal abundance (log-transformed) and algal cell size. Because all non-spherical algal morphotypes were observed at low abundance, they were pooled and treated as a single category ("non-spherical cells") for subsequent analyses. Redundancy analysis (RDA) based on Hellinger-transformed community composition data was used to examine the relationships between algal community structure and environmental variables. The significance of the overall model, constrained axes, and explanatory variables was assessed using permutation tests. All analyses were conducted using R software (R Core Team 2024).

3 Results

3.1 Red snow algae in snow samples

Microscopic observations revealed that the red snow samples contained snow algae of various sizes and morphotypes (Fig. 3). The observed algae were classified into five distinct morphotypes: (1) spherical cells of various sizes (Fig. 3a); (2) spherical cells with a stalk-like protrusion (Fig. 3b), with a cell diameter of 21.3 ± 8.0 µm (mean ± SD); (3) elliptical cells (Fig. 3d), with a length of 20.1 ± 2.5 µm and a width of 11.3 ± 1.0 µm; (4) oval shaped cells (Fig. 3c), a length of 31.3 ± 7.2 µm and a width of 26.3 ± 7.2 µm; (5) oval shaped cells with a ribbed cell wall (Fig. 3e), with a cell length of 24.8 ± 2.6 µm and a cell width of 15.3 ± 2.3 µm.

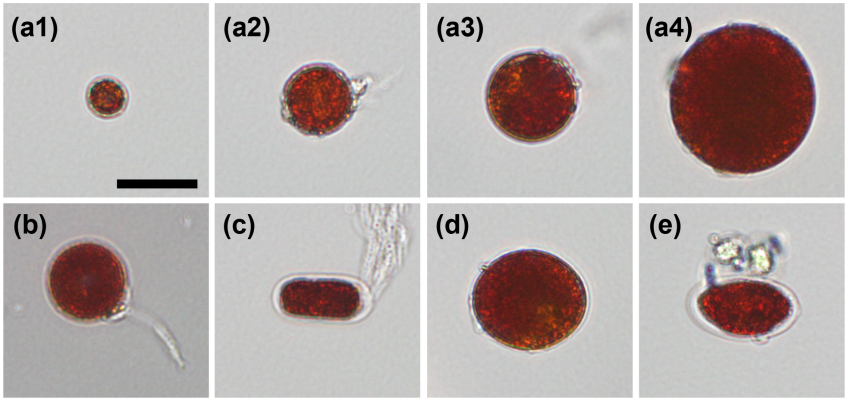

Figure 3: Microphotographs of red snow algae observed in this study. (a1)–(a4) Spherical cells of different sizes. (b) Spherical cell with a stalk-like protrusion. (c) Elliptical cell. (d) Oval-shaped cell. (e) Oval-shaped cells with ribbed cell walls and non-spherical cells. A scale bar is 20 µm.

https://doi.org/10.5194/egusphere-2026-2789
Preprint. Discussion started: 5 June 2026

3.2 Distributions in snow algal assemblages on the snow surface

Algal abundances on the snow surface showed different spatial patterns between spherical and non-spherical morphotypes (Fig. 4). Spherical cells were observed across both ice-based and soil-based snowpack, and their mean concentrations were similar between the two environments ($2.6 \pm 1.1 \times 10^4$ cells mL^{-1} in ice-based snowpack and $2.6 \pm 1.4 \times 10^4$ cells mL^{-1} in soil-based snowpack; Dunn's test, $p = 0.818$). By contrast, non-spherical cells were observed more consistently in soil-based snowpack and lower ice-based sites (S1–S20) than in upper ice-based sites (S21–S30). Among the non-spherical morphotypes, elliptical cells accounted for the majority of observed cells, and their mean concentration was significantly higher in soil-based snowpack ($1.9 \pm 1.3 \times 10^3$ cells mL^{-1}) than in ice-based snowpack ($1.3 \pm 1.9 \times 10^3$ cells mL^{-1}; Dunn's test, $p = 0.041$).

The size distribution of spherical cells also differed between the two underlying environments (Figs. 4, 5). In ice-based snowpack, mean size of spherical cell was 13.9 ± 2.5 μm, and most sites were dominated by cells with diameters of 8–12 μm, although an additional peak at 14–24 μm was observed at several sites. In soil-based snowpack, larger spherical cells were more frequent, with a mean size of 20.4 ± 3.7 μm. Size distributions there commonly showed peaks not only at 12–24 μm but also at larger diameters (28–40 μm). Consequently, mean size of spherical cell differed significantly between ice-based and soil-based snowpack (Dunn's test, $p = 0.009$).

3.3 Differences between surface and subsurface layers in algal abundance and size of spherical cell in the ice-based snowpack

Within ice-based snowpack, the contrast between the surface and subsurface varied along the glacier valley in a downstream-to-upstream direction (Fig. 4). At lower sites (S11–S19), spherical cell concentration was higher on the snow surface than in the subsurface, whereas at upper sites (S20–S30), concentrations were broadly similar between the two layers. Non-spherical cells were detectable in the subsurface at lower sites (S11–S20) but were rarely observed in the subsurface at upper sites (S21-S30), while surface concentrations remained higher overall. Despite these local differences, the overall difference in spherical cell concentration between the surface and subsurface was not significant (Dunn's test, $p = 0.074$), whereas the difference for elliptical cells was significant (Dunn's test, $p = 0.041$).

The direction of layer differences in spherical cell size differed from that in cell concentration (Figs. 4, 5). At lower to middle sites (S11-S23), spherical cells on the snow surface were consistently larger than those in the subsurface. In contrast, at upper sites (S24-S30), mean size of spherical cell was similar between the surface and subsurface. Overall, spherical cells were significantly larger on the snow surface than within the snowpack (Dunn's test, $p = 0.009$).

https://doi.org/10.5194/egusphere-2026-2789
Preprint. Discussion started: 5 June 2026

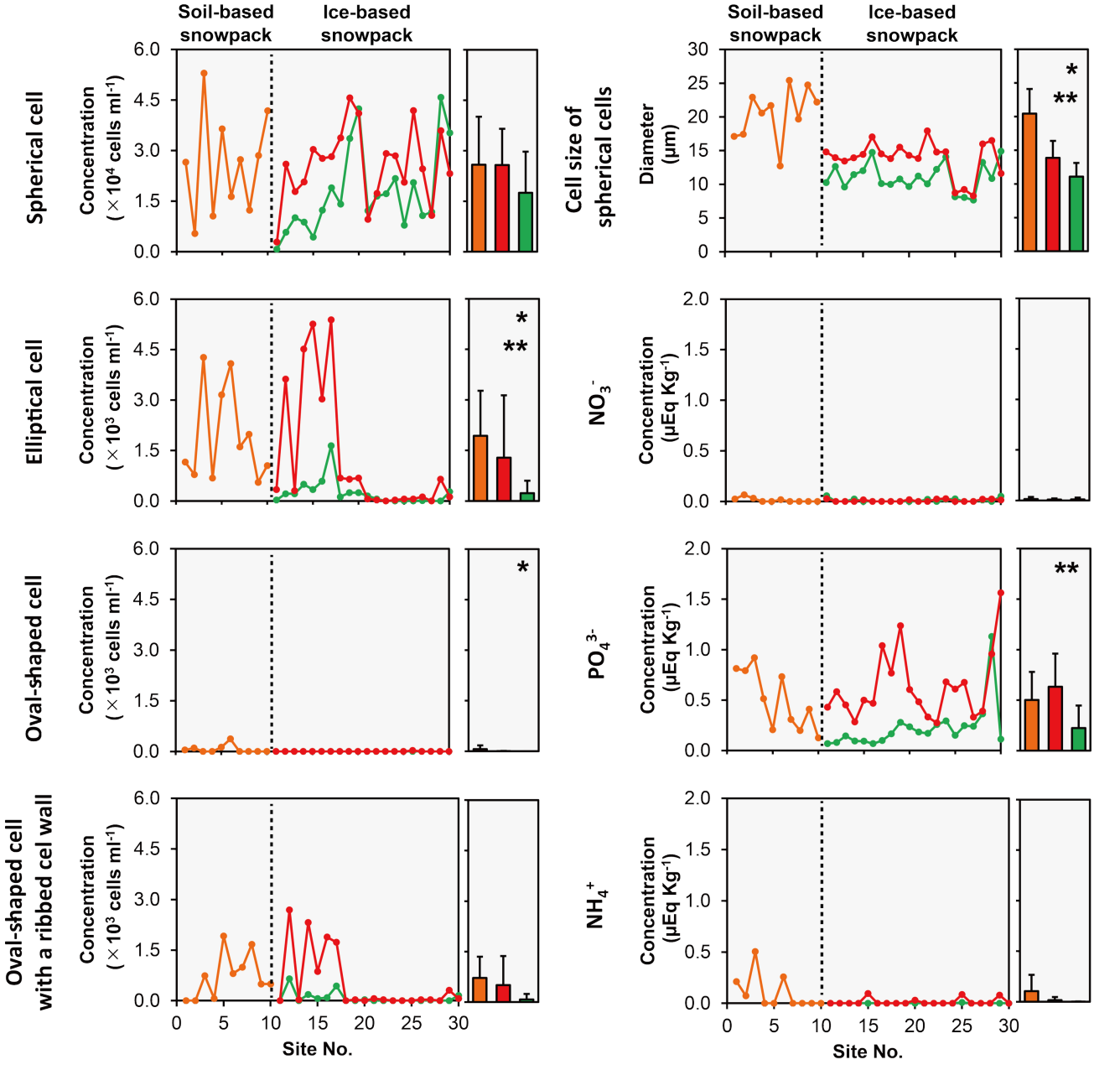

Figure 4: Spatial variability of algal abundance, size of spherical cell, and nutrient concentrations. Spatial distributions are shown in the left panels, and comparisons among the on-glacier snowpack (surface and subsurface) and the glacier forefield (snow surface) are shown in the right panels. * indicates a significant difference between the on-glacier snowpack and the glacier forefield (Dunn's test, $p < 0.05$), and ** indicates a significant difference between the surface and subsurface within the on-glacier snowpack (Dunn's test, $p < 0.05$).

https://doi.org/10.5194/egusphere-2026-2789
Preprint. Discussion started: 5 June 2026

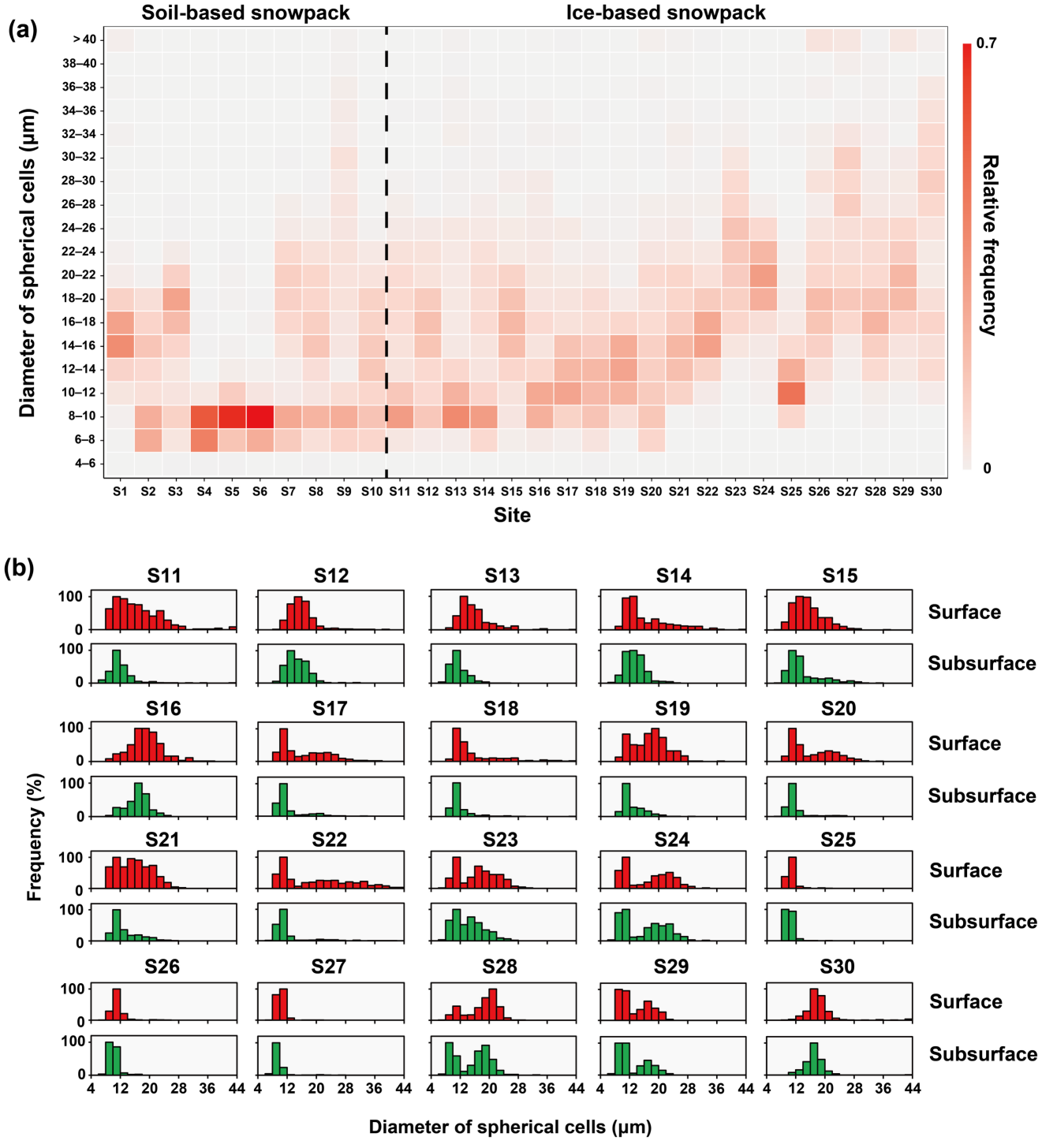

Figure 5: Size distribution of spherical cells (a) Size distribution of spherical cells on the snow surface. (b) Histograms of size of spherical cells on the surface and subsurface within ice-based snowpack. Frequency is expressed as relative frequency, with the most frequently observed size class in each sample set normalized to 100%.

https://doi.org/10.5194/egusphere-2026-2789
Preprint. Discussion started: 5 June 2026

3.4 Spatial variation in microbial community structure in 18S rRNA analysis

After quality filtering and chimera removal, a total of 386,368 high-quality 18S rRNA reads were obtained from the snow samples, with an average of 29,721 reads per sample. In red snow samples, mainly four phyla were dominated: Chlorophyte, Ascomycote, Basidiomycote, and Cercozoa (Figs. 6a, 7a).

The community structure of Chlorophyta associated with red snow varied systematically from downstream to upstream (Figs. 6b, c, 7b, c). In this study area, the Chlorophyta community was dominated by four genera: *Sanguina*, *Rosetta*, *Chloromonas*, and *Raphidonema* (Figs. 6b, 7b). Focusing on taxa potentially responsible for red pigmentation (*Sanguina*, *Rosetta*, and *Chloromonas*; Figs. 6c, 7c), clear spatial shifts in relative abundance were observed. In soil-based snowpack (S1, S4, S7, S9, S10), *Sanguina* accounted for 32–82% of the community, while *Rosetta* and *Chloromonas* also contributed substantially (3–34% and 4–22%, respectively).

Within the ice-based snowpack, the subsurface snow exhibited an altitudinal pattern broadly similar to that observed in the surface snow. *Chloromonas* was more abundant in the lower part of the ice-based snowpack, whereas *Sanguina* remained dominant at upper sites.

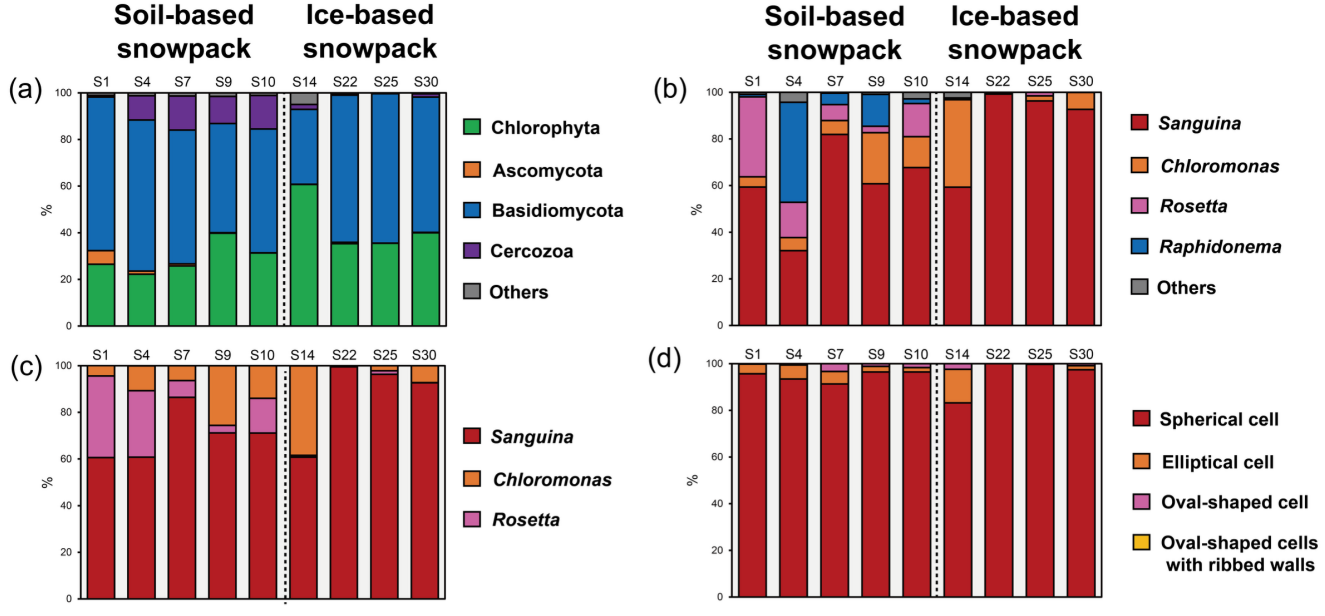

Figure 6: Microbial community structure on the snow surface based on 18S rRNA gene sequencing and morphological observations. Community structure at each elevation is presented as stacked bar charts normalized to 100%. (a) Overall community structure based on 18S rRNA sequencing. (b) Community structure restricted to Chlorophyta. (c) Algal community structure focusing on chlorophyte genera potentially responsible for red pigmentation. (d) Relative abundance of algal morphotypes calculated from cell concentrations. For the molecular dataset, only phyla or genera accounting for >5% of the total reads were included in the analysis.

https://doi.org/10.5194/egusphere-2026-2789
Preprint. Discussion started: 5 June 2026

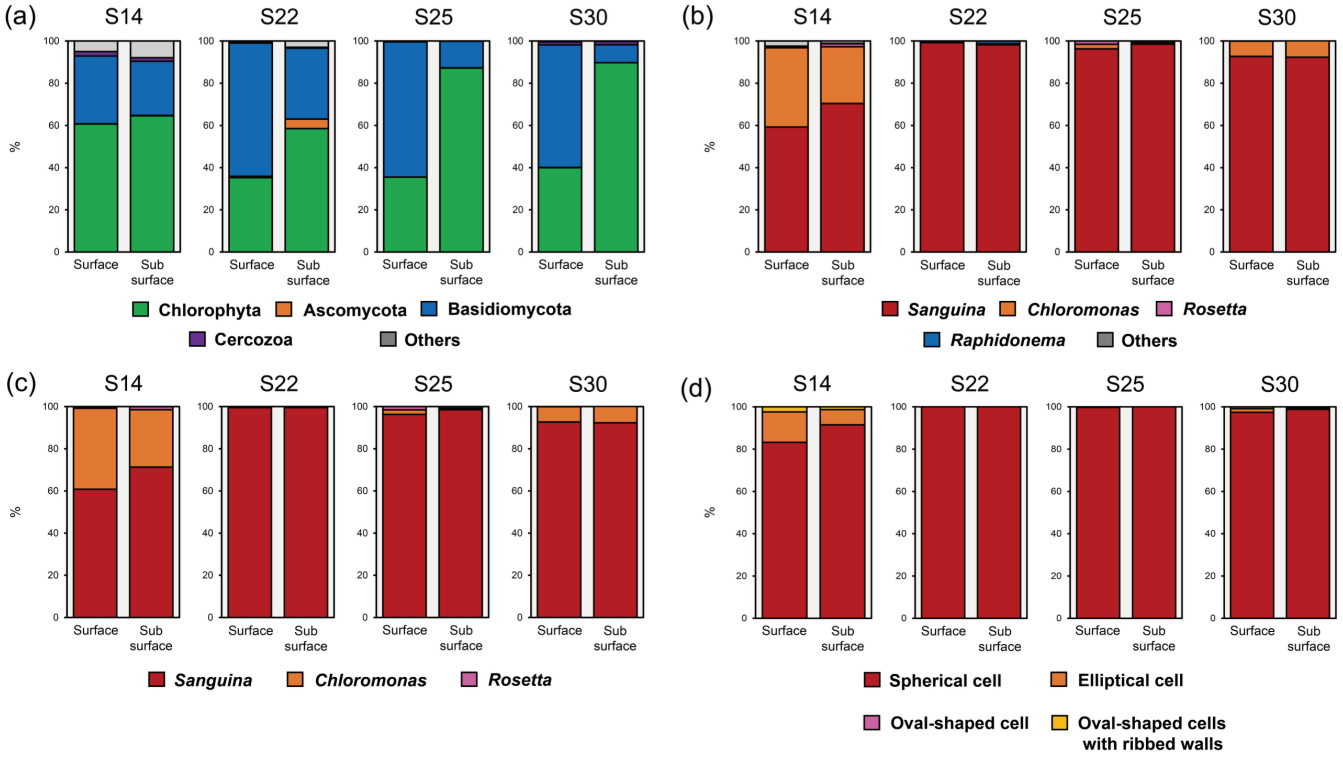

Figure 7: Microbial community structure on the surface and subsurface in ice-based snowpack. Community structure is presented as stacked bar charts normalized to 100% for each site, comparing the snow surface (left) and snow subsurface (right) across four sites. Panels (a–d) correspond to the same classifications as in Fig. 6: (a) overall community structure based on 18S rRNA gene sequencing, (b) community structure restricted to Chlorophyta, (c) chlorophyte genera potentially responsible for red pigmentation, and (d) relative abundance of algal morphotypes based on cell concentrations. For the molecular dataset, only phyla or genera accounting for >5% of the total reads were included.

3.5 Spatial variability in nutrients in snowpacks

Among the soluble nutrients measured, PO_4^{3-} was the only species consistently detected across all sites, while dissolved inorganic nitrogen (NO_3^- and NH_4^+) was extremely scarce (< 0.1 µEq kg^{-1}) regardless of the underlying environment or depth (Fig. 4). The only exception was slightly elevated NH_4^+ (0.2–0.5 µEq kg^{-1}) found on the snow surface at a few downstream sites (S2, S3, and S5).

Regarding spatial distribution across the glacier, PO_4^{3-} concentrations on the snow surface ranged from 0.1 to 1.6 µEq kg^{-1} and showed no significant difference between soil-based and ice-based snowpacks (Dunn's test, $p = 0.351$). However, within the ice-based snowpack, a distinct elevational trend was observed: PO_4^{3-} levels were significantly higher at the upper sites (S18–S30; 0.1–1.1 µEq kg^{-1}) compared to the lower and middle sites (S11–S17; ≤ 0.1 µEq kg^{-1}).

Comparisons between surface and subsurface in the ice-based snowpack revealed that nutrient availability was predominantly higher at the surface. Across all ice-based sites, surface PO_4^{3-} concentrations were significantly higher than those in the

https://doi.org/10.5194/egusphere-2026-2789
Preprint. Discussion started: 5 June 2026

subsurface, averaging 4.3 ± 3.3 times greater (Dunn's test, $p < 0.001$). Inorganic nitrogen followed a pattern similar to that of the snow surface, with subsurface concentrations remaining below 0.1 μEq kg^{-1} across all sampling sites.

4 Discussion

4.1 Relationship between morphotypes assemblages and algal community structure

The combined morphological observations and molecular analyses show that morphotype assemblages in red snow are partially consistent with 18S rRNA-based algal community structure, but the strength of this correspondence differs among morphotypes. Across the glacier valley, the higher relative abundances of *Chloromonas* and *Rosetta* at soil-based and lower ice-based sites, and the dominance of *Sanguina* at upper ice-based sites, were reflected spherical cell in the morphotype data, with greater contributions of *Chloromonas* and *Rosetta* corresponding to a higher proportion of non-spherical cells (Fig. 6c, d).

At the same time, the comparison between microscopy and molecular analysis reveals an important mismatch between morphology and taxonomy. At several sites, spherical cells remained the dominant morphotype even when the algal community included substantial contributions from *Chloromonas* and *Rosetta* (Figs. 6c, d, 7c, d). This indicates that the spherical morphotype is taxonomically heterogeneous and cannot be interpreted as a single lineage. Previous studies support this explanation. *Sanguina nivaloides* is typically observed as spherical cells during blooms and is widely distributed across polar and alpine snowpacks (Segawa *et al.* 2018; Procházková *et al.* 2019). In contrast, *Chloromonas* and *Rosetta* include multiple cell forms, including spherical or nearly spherical stages depending on species and life stage (Novakovskaya *et al.* 2018; Engstrom *et al.* 2024; Procházková *et al.* 2024). Therefore, morphology alone can merge taxonomically distinct algae into the same category, especially for spherical cells.

This mismatch is important for interpreting spatial variability in red snow. Morphological observations are useful for describing visible morphotype assemblages, whereas 18S rRNA-based analyses are required to resolve which taxa contribute to those assemblages. In the present study, the clearest example is the spherical morphotype, which includes both Sanguina-rich assemblages and mixed assemblages containing greater contributions from *Chloromonas* and *Rosetta*. Accordingly, shifts in morphology should be interpreted together with taxonomic data rather than as direct proxies for species composition.

4.2 Factors controlling algal community structure along the glacier valley

Redundancy analysis (RDA), conducted for algal community structure, identified elevation, snow depth, and nutrients as candidate explanatory variables (Fig. 8). The constrained model explained 72.2% of the total variance, with an adjusted R^2 of 0.555. Among the constrained axes, only RDA1 was significant ($F = 9.41$, $p = 0.009$), whereas RDA2 was not significant ($F = 3.53$, $p = 0.187$). Sequential permutation tests indicated that snow depth ($F = 6.24$, $p = 0.009$) and elevation ($F = 6.61$, $p = 0.006$) significantly explained community variation, whereas nutrients did not ($F = 0.12$, $p = 0.907$). These results indicate that the principal controls on algal community structure were associated with physical progression of melt rather than bulk nutrient concentrations alone.

https://doi.org/10.5194/egusphere-2026-2789
Preprint. Discussion started: 5 June 2026

Elevation likely represents a gradient in the timing and duration of snowmelt along the valley. In the present dataset, soil-based and lower ice-based sites contained higher relative abundances of *Chloromonas* and *Rosetta*, whereas upper ice-based sites were strongly dominated by *Sanguina*. A similar explanation has been proposed for Gulkana Glacier, where snow algal species distributions varied with altitude and presumably with melt progression (Takeuchi 2001, 2013). Because *Sanguina* is a widespread constituent of red snow communities and can colonize melting snow surfaces broadly across alpine and polar environments (Segawa *et al.* 2018; Procházková *et al.* 2019; Hoham & Remias 2020), its dominance at higher-elevation sites may reflect earlier-stage or less-developed habitats along the seasonal melt gradient.

Snow depth provides a second key control because it governs connectivity between the illuminated snow surface and potential local cell reservoirs below. Snow depth is often related to elevation, with lower-elevation sites typically exhibiting shallower snowpacks due to enhanced melt and longer exposure periods (Anderton *et al.* 2004; Clark *et al.* 2011). In our study, such a relationship was partially observed within the ice-based snowpack (e.g., S18–S26, Fig. 1c), where snow depth decreased with decreasing elevation. However, this pattern was not consistent across all sites, indicating that local variability in snow accumulation and melt conditions can decouple snow depth from elevation. These results suggest that snow depth acts as an additional control that cannot be fully explained by elevation alone. Recent experimental work on the Harding Icefield showed that red snow blooms can be strongly influenced by cysts resurfacing from subsurface snow and firn, rather than by passive atmospheric deposition alone (Rea & Dial 2024). Likewise, life-cycle syntheses for snow algae indicate that cells retained deeper in snow or at the snow-substrate interface can become available as meltwater increases pore connectivity (Hoham & Duval 2001; Matsumoto *et al.* 2024). Within this framework, shallower or more melted snowpacks at soil-based and lower ice-based sites may more readily connect the snow surface with subsurface or boundary-associated sources, whereas deeper snowpacks at upper sites may delay upward supply from local reservoirs. This is consistent with our vertical sampling, which showed stronger surface-subsurface contrasts at lower ice-based sites than at upper sites.

Nutrients, by contrast, did not show a significant independent effect in the RDA, and dissolved inorganic nitrogen was rarely detected at most sites. This suggests that the broad spatial turnover in algal community structure was not primarily determined by concentrations of dissolved NO_3^- and NH_4^+ at the time of sampling. However, nutrients may still modulate local growth or life-stage transitions once taxa reach the surface. PO_4^{3-} was consistently detected and was higher on the snow surface than in the subsurface, indicating that nutrient conditions differ vertically within the snowpack, but those differences were secondary to elevation and snow depth in explaining among-site community variation.

The substrate under the snowpacks (i.e. ice or soil) also appears to matter, although it is partly intertwined with snow depth and melt stage. Soil-based snowpack in downstream contained more non-spherical cells, larger spherical cells, and more mixed taxonomic communities than ice-based snowpack. This pattern is consistent with the idea that the environment beneath the snow influences which local source populations can enter the snowpack during melt. In soil-based snowpack, the snow-ground interface may provide an additional reservoir of locally retained cells and cysts, as proposed for snow algae associated with terrestrial substrates and snow-ground boundaries (Hoham & Duval 2001; Matsumoto *et al.* 2024). In ice-based snowpack, by contrast, likely source environments include retained cells in subsurface snow, firn, or the glacier surface (Hoham & Duval

https://doi.org/10.5194/egusphere-2026-2789
Preprint. Discussion started: 5 June 2026

2001; Matsumoto *et al.* 2024). Direct source tracing was beyond the scope of this study, so we cannot conclude whether substrate type itself or the shallower, more melt-advanced conditions of downstream snowpack are the dominant cause. Nevertheless, the observed differences indicate that whether the snow overlies ice or soil is not neutral for red snow community development.

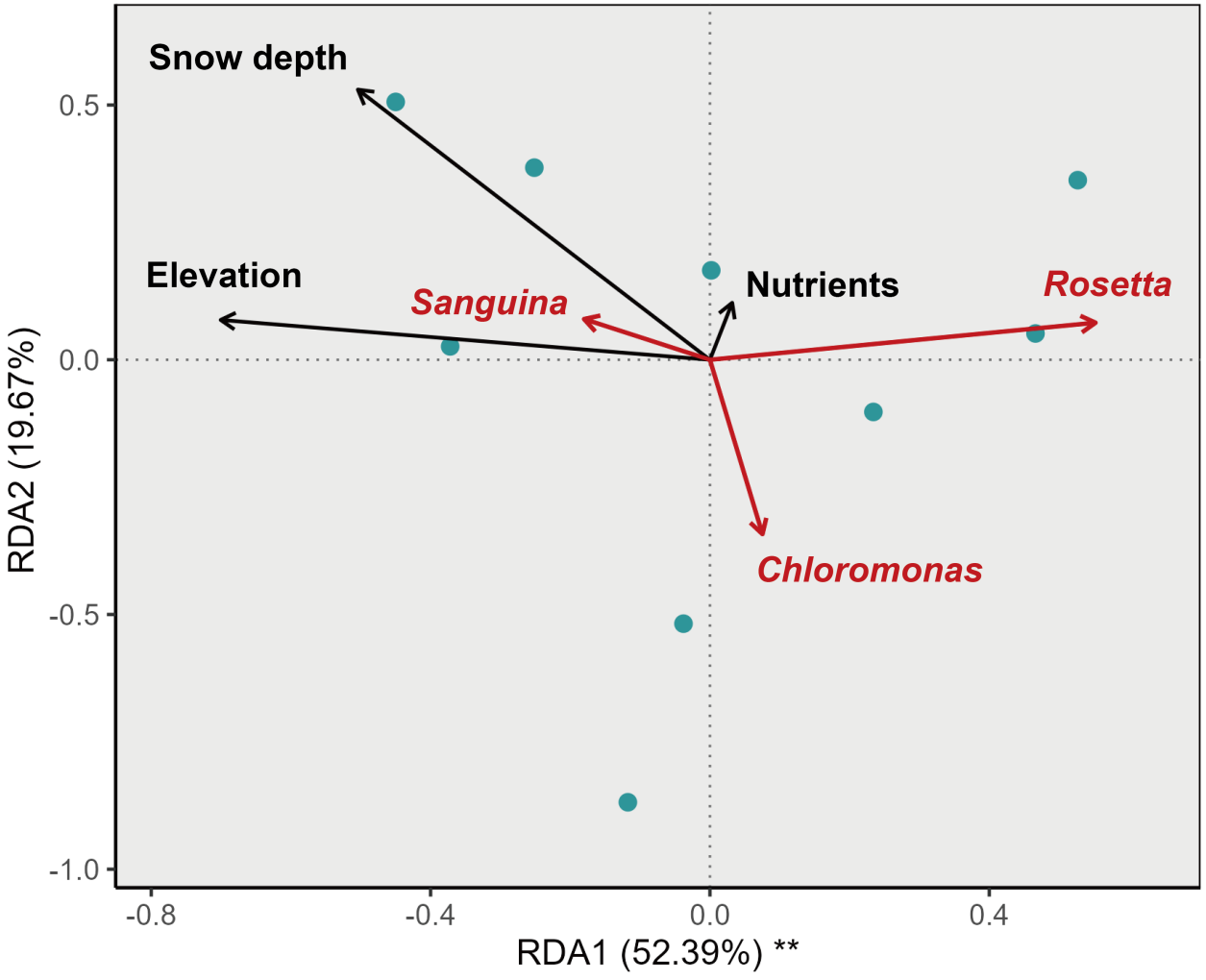

Figure 8: Redundancy analysis (RDA) biplot of algal community composition based on Hellinger-transformed relative abundance data. Blue points indicate sampling sites. Black arrows indicate environmental variables included in the RDA, and red arrows indicate the directions of algal taxa in the ordination space. Percentages on the axes represent the proportion of total variance explained by each constrained axis. Asterisks indicate the significance of each axis based on permutation tests ($P < 0.05$, P < 0.01, $P < 0.001$).

https://doi.org/10.5194/egusphere-2026-2789
Preprint. Discussion started: 5 June 2026

4.3 Factors controlling size of spherical cell and interpretation of the spherical morphotype

The microscopic and molecular analysis results show that the spherical morphotype includes multiple taxa, suggesting that variation in size of spherical cell cannot be attributed solely to life-cycle progression within a single species. Instead, the observed size distribution (Fig. 5) likely reflects two overlapping processes: changes in the taxonomic composition contained within the spherical cells and size variation within taxa across life stages and environmental conditions. This means a shift toward larger spherical cells at a site does not necessarily indicate only growth or maturation of *Sanguina*; it may also reflect increasing contributions of other taxa that are included within the spherical morphotype.

Even so, the observed environmental pattern in spherical cell size suggests that within-taxon variation may also contribute. Spherical cells were larger in soil-based snowpack and at the snow surface, and elevation was a significant predictor at the surface (Table 1). If elevation reflects melt timing, this pattern is consistent with progressive cell enlargement during melt, as reported for *Sanguina nivaloides* (Remias *et al.* 2005; Procházková *et al.* 2019).

Cell size is also important because it can influence the albedo effect of red snow blooms. Larger spherical cells generally contain more pigment per cell and may therefore contribute more strongly to snow darkening where they occur at high abundance (Halbach *et al.* 2022; Chevrollier *et al.* 2023). The observed tendency for larger cells in the soil-based snowpack and at the surface suggests that the radiative impact of blooms varies spatially along the glacier valley. Specifically, the presence of larger cells, combined with high cell abundance, likely exacerbates albedo reduction, as larger and more pigmented cells can enhance bulk light absorption, given that algal optical properties depend on cell size, pigmentation, and intracellular light scattering (Cook *et al.* 2020; Halbach *et al.* 2022). Consequently, the soil-based snowpack at lower elevations may experience more pronounced biological snowmelt than the ice-based snowpack due to this shift in cell size structure.

Table 1: Results of generalized linear models (GLMs) examining the relationships between environmental variables and, spherical cell concentration, non-spherical cell concentration, and size of spherical cell in (a) snow surface and (b) subsurface. Bold values indicate statistically significant predictors (p < 0.05).

(a)

Cell size of spherical cells (surface snow)

Predictor	Estimate	SE	t	p	95% CI
Snow depth	-0.009	0.012	-0.752	0.459	-0.033 – 0.016
Elevation	**-0.010**	**0.004**	**-2.622**	**0.014**	**-0.018 – -0.002**
Nutrients	-1.841	1.660	-1.109	0.278	-5.253 – 1.571

Non-spherical cell (log, surface snow)

Predictor	Estimate	SE	t	p	95% CI
Snow depth	**-0.016**	**0.006**	**-2.557**	**0.017**	**-0.029 – -0.003**
Elevation	-0.002	0.002	-0.964	0.344	-0.006 – 0.002
Nutrients	1.119	0.888	1.260	0.219	-0.706 – 2.943

Spherical cell (log, surface snow)

Predictor	Estimate	SE	t	p	95% CI
Snow depth	0.001	0.002	0.545	0.590	-0.004 – 0.006
Elevation	0.000	0.001	0.176	0.862	-0.001 – 0.002
Nutrients	0.356	0.330	1.080	0.290	-0.322 – 1.035

(b)

Cell size of spherical cells (subsurface snow)

Predictor	Estimate	SE	t	p	95% CI
Snow depth	-0.014	0.008	-1.878	0.079	-0.030 – 0.002
Elevation	0.005	0.005	0.995	0.335	-0.006 – 0.017
Nutrients	-0.524	2.425	-0.216	0.832	-5.665 – 4.617

Non-spherical cell (log, subsurface snow)

Predictor	Estimate	SE	t	p	95% CI
Snow depth	**-0.019**	**0.007**	**-2.706**	**0.016**	**-0.034 – -0.004**
Elevation	-0.003	0.005	-0.589	0.564	-0.013 – 0.008
Nutrients	**-5.156**	**2.236**	**-2.306**	**0.035**	**-9.896 – -0.416**

Spherical cell (log, subsurface snow)

Predictor	Estimate	SE	t	p	95% CI
Snow depth	0.001	0.003	0.430	0.673	-0.004 – 0.007
Elevation	**0.005**	**0.002**	**2.530**	**0.022**	**0.001 – 0.009**
Nutrients	0.585	0.845	0.692	0.499	-1.207 – 2.377

https://doi.org/10.5194/egusphere-2026-2789
Preprint. Discussion started: 5 June 2026

4.4 Vertical distribution of red snow algae within the snowpack and its implications for bloom development

The comparison between surface (0–5 cm) and subsurface (5–10 cm) layers demonstrates that red snow algae are not confined to the snow surface but maintain a substantial biomass within the snowpack. In the ice-based snowpack, spherical cell concentrations at lower and middle sites (S11–S17) were significantly higher in the subsurface than at the surface ($p < 0.05$), whereas no such difference was observed at upper sites (S18–S30). This pattern suggests that, as snowmelt progresses at lower elevations, algae distributed within the snowpack are redistributed toward the surface, while the subsurface acts as a persistent reservoir that sustains bloom development (Ono et al., 2025).

The observed taxonomic differentiation between layers further supports this mechanism. Although *Sanguina* was present in both layers, the relative abundance of *Chloromonas* was higher at the surface, implying that species-specific traits, such as motility or adaptation to higher light conditions, may promote preferential accumulation in the upper layer and thereby influence the composition of visible blooms. In contrast, for the soil-based snowpack, the absence of subsurface data precludes direct evaluation of whether surface blooms originate from internal snowpack populations or from resting stages in the underlying soil. While the ice-based sites indicate a clear contribution from a subsurface reservoir, the extent to which substrate conditions control colonization and bloom initiation in soil-based environments remains unresolved.

5 Conclusions

In this study, combined morphological observations and molecular analyses showed that red snow varies systematically along a glacial valley in Alaska in both morphotype assemblage and algal community structure. Redundancy analysis demonstrated that this spatial variability was explained primarily by snow depth and elevation, whereas nutrients did not show a significant independent effect. These results indicate that community turnover along the valley is governed mainly by a snowmelt-driven environmental gradient, with soil-based and lower ice-based sites representing relatively more melted habitats that favor mixed communities with greater contributions from *Chloromonas* and *Rosetta*, whereas deeper and higher-elevation snowpacks in the upper ice-based sites represent relatively less-developed habitats. At the same time, differences in community structure and size of spherical cells between ice-based and soil-based snowpack suggest that the environment beneath the snow also contributes to community development, most likely because melt progression changes how readily locally retained cells at subsurface or snow-substrate boundaries can reach the snow surface. We also found that spherical cells were taxonomically heterogeneous, indicating that morphology alone can obscure community shifts, and that bloom development involves vertical redistribution within the snowpack rather than only processes at the visible surface. Together, these results provide a framework for understanding red snow heterogeneity as the outcome of snowmelt progression, source-environment differences beneath the snow, and vertical development within the snowpack.

https://doi.org/10.5194/egusphere-2026-2789
Preprint. Discussion started: 5 June 2026

Code and data availability

The datasets generated and analyzed during the current study are available from the corresponding author upon reasonable request.

Author contributions

Sampling for research: MO, KK, RA; manuscript conception: MO and NT; microscopy: MO; DNA analysis: KK, JU; chemical analysis: MO; and statistical analysis: MO. All authors have edited and reviewed the manuscript.

Competing interests

The contact author has declared that none of the authors has any competing interests.

Disclaimer

Copernicus Publications remains neutral with regard to jurisdictional claims made in the text, published maps, institutional affiliations, or any other geographical representation in this paper. While Copernicus Publications makes every effort to include appropriate place names, the final responsibility lies with the authors. Views expressed in the text are those of the authors and do not necessarily reflect the views of the publisher.

Acknowledgements

We sincerely thank Roman Dial and Peggy Dial for their invaluable support during our stay in Alaska. Generative AI tools were used for English language refinement during manuscript preparation. All scientific interpretations and conclusions were made by the authors.

Financial support

This research has been supported by JSPS KAKENHI (grant nos. 20K21840, 20H00196, 21H03612, 22J11017, 22KJ0471, 24KJ0118, and 25K21373) and the Arctic Challenge for Sustainability II (ArCS II, Program grant no. JPMXD1420318865).

References

Almela, P., Elser, J. J., Giersch, J. J., Hotaling, S., & Hamilton, T. L. (2025). Influence of snow cover on albedo reduction by snow algae. *mBio*, **16**(2), e03630-24.

https://doi.org/10.5194/egusphere-2026-2789
Preprint. Discussion started: 5 June 2026

Anderton, S. P., White, S. M., & Alvera, B. (2004). Evaluation of spatial variability in snow water equivalent for a high mountain catchment. *Hydrological Processes*, **18**(3), 435–453.

Barnett, D., Arts, I., & Penders, J. (2021). microViz: an R package for microbiome data visualization and statistics. *Journal of Open Source Software*, **6**(63), 3201.

Callahan, B. (2018, February 13). Silva Taxonomic Training Data Formatted For Dada2 (Silva Version 132), Zenodo. doi:10.5281/ZENODO.1172783

Callahan, B. J., McMurdie, P. J., Rosen, M. J., Han, A. W., Johnson, A. J. A., & Holmes, S. P. (2016). DADA2: High-resolution sample inference from Illumina amplicon data. *Nature Methods*, **13**(7), 581–583.

Cheung, M. K., Au, C. H., Chu, K. H., Kwan, H. S., & Wong, C. K. (2010). Composition and genetic diversity of picoeukaryotes in subtropical coastal waters as revealed by 454 pyrosequencing. *The ISME Journal*, **4**(8), 1053–1059.

Chevrollier, L.-A., Cook, J. M., Halbach, L., … Tranter, M. (2023). Light absorption and albedo reduction by pigmented microalgae on snow and ice. *Journal of Glaciology*, **69**(274), 333–341.

Clark, M. P., Hendrikx, J., Slater, A. G., … Woods, R. A. (2011). Representing spatial variability of snow water equivalent in hydrologic and land-surface models: A review. *Water Resources Research*, **47**(7), 2011WR010745.

Cook, J. M., Hodson, A. J., Gardner, A. S., … Tranter, M. (2017). Quantifying bioalbedo: a new physically based model and discussion of empirical methods for characterising biological influence on ice and snow albedo. *The Cryosphere*, **11**(6), 2611–2632.

Cook, J. M., Tedstone, A. J., Williamson, C., … Tranter, M. (2020). Glacier algae accelerate melt rates on the south-western Greenland Ice Sheet. *The Cryosphere*, **14**(1), 309–330.

Engstrom, C. B., Raymond, B. B., Albeitshawish, J., Bogdanovic, A., & Quarmby, L. M. (2024). *Rosetta* gen. nov. (Chlorophyta): Resolving the identity of red snow algal rosettes. *Journal of Phycology*, **60**(2), 275–298.

Fiołka, M. J., Takeuchi, N., Sofińska-Chmiel, W., Mieszawska, S., & Treska, I. (2020). Morphological and physicochemical diversity of snow algae from Alaska. *Scientific Reports*, **10**(1), 19167.

Halbach, L., Chevrollier, L.-A., Doting, E. L., … Anesio, A. M. (2022). Pigment signatures of algal communities and their implications for glacier surface darkening. *Scientific Reports*, **12**(1), 17643.

Hoham, R. W., & Duval, B. (2001). *Microbial ecology of snow and freshwater ice Snow Ecology*, Cambridge: Cambridge University Press.

Hoham, R. W., & Remias, D. (2020). Snow and Glacial Algae: A Review. *Journal of Phycology*, **56**(2), 264–282.

Hotaling, S., Lutz, S., Dial, R. J., … Hamilton, T. L. (2021). Biological albedo reduction on ice sheets, glaciers, and snowfields. *Earth-Science Reviews*, **220**, 103728.

Kol, E. (1968). Kol, Erzsébet. "Kryobiologie. Biologie und limnologie des schnees und eises. I. Kryovegetation. *Schweizerbart'sche Verlagsbuchhandlung*.

Lutz, S., Anesio, A. M., Raiswell, R., … Benning, L. G. (2016). The biogeography of red snow microbiomes and their role in melting arctic glaciers. *Nature Communications*, **7**(1), 11968.

https://doi.org/10.5194/egusphere-2026-2789
Preprint. Discussion started: 5 June 2026

Matsumoto, M., Hanneman, C., Camara, A. G., Krueger-Hadfield, S. A., Hamilton, T. L., & Kodner, R. B. (2024). Hypothesized life cycle of the snow algae *Chlainomonas* sp. (Chlamydomonadales, Chlorophyta) from the Cascade Mountains, USA. *Journal of Phycology*, **60**(3), 724–740.

McMurdie, P. J., & Holmes, S. (2013). phyloseq: An R Package for Reproducible Interactive Analysis and Graphics of Microbiome Census Data. *PLoS ONE*, **8**(4), e61217.

Muller, T., Bleiss, W., Matin, C. D., Rogaschewski, S., & Fuhr, G. (1998). Snow algae from northwest Svalbard: their identification, distribution, pigment and nutrient content. *Polar Biol.*, **20**, 14–32.

Nakashima, T., Uetake, J., Segawa, T., Procházková, L., Tsushima, A., & Takeuchi, N. (2021). Spatial and Temporal Variations in Pigment and Species Compositions of Snow Algae on Mt. Tateyama in Toyama Prefecture, Japan. *Frontiers in Plant Science*, **12**, 689119.

Novakovskaya, I. V., Patova, E. N., Boldina, O. N., Patova, A. D., & Shadrin, D. M. (2018). Molecular Phylogenetic Analyses, Ecology and Morphological Characteristics of *Chloromonas reticulata* (Goroschankin) Gobi Which Causes Red Blooming of Snow in the Subpolar Urals. *Cryptogamie, Algologie*, **39**(2), 199–213.

Novis, P. M. (2002). Ecology of the snow alga Chlainomonas kolii (Chlamydomonadales, Chlorophyta) in New Zealand. *Phycologia*, **41**(3), 280–292.

O'Neel, S., McNeil, C., Sass, L. C., … Fagre, D. (2019). Reanalysis of the US Geological Survey Benchmark Glaciers: long-term insight into climate forcing of glacier mass balance. *Journal of Glaciology*, **65**(253), 850–866.

Ono, M., Kobayashi, K., Seto, D., … Takeuchi, N. (2025). Temporal and vertical changes in snow microbial communities during the melting season below canopy in Northern Japan. *The Cryosphere*, **19**(11), 5983–5999.

Procházková, L., Leya, T., Křížková, H., & Nedbalová, L. (2019). Sanguina nivaloides and Sanguina aurantia gen. et spp. nov. (Chlorophyta): the taxonomy, phylogeny, biogeography and ecology of two newly recognised algae causing red and orange snow. *FEMS Microbiology Ecology*, **95**(6), fiz064.

Procházková, L., Remias, D., Holzinger, A., Řezanka, T., & Nedbalová, L. (2018). Ecophysiological and morphological comparison of two populations of *Chlainomonas* sp. (Chlorophyta) causing red snow on ice-covered lakes in the High Tatras and Austrian Alps. *European Journal of Phycology*, **53**(2), 230–243.

Procházková, L., Remias, D., Suzuki, H., Kociánová, M., & Nedbalová, L. (2024). *Chloromonas rubrosalmonea* sp. nov. (Chlorophyta) causes blooms of salmon-red snow due to high astaxanthin and low chlorophyll content. *Botany Letters*, 1–19.

R Core Team. (2024). R: A language and environment for statistical computing. *R Foundation for Statistical Computing, Vienna, Austria*. Retrieved from https://www.R-project.org/

Rea, M. E., & Dial, R. J. (2024). An experimental assessment of active and passive dispersal of red snow algae on the Harding Icefield, southcentral Alaska. *Arctic, Antarctic, and Alpine Research*, **56**(1), 2370905.

Remias, D., Lütz-Meindl, U., & Lütz, C. (2005). Photosynthesis, pigments and ultrastructure of the alpine snow alga *Chlamydomonas nivalis*. *European Journal of Phycology*, **40**(3), 259–268.

https://doi.org/10.5194/egusphere-2026-2789
Preprint. Discussion started: 5 June 2026

Roussel, L., Dumont, M., Gascoin, S., … Maréchal, E. (2024). Snowmelt duration controls red algal blooms in the snow of the European Alps. *Proceedings of the National Academy of Sciences*, **121**(41), e2400362121.

Segawa, T., Matsuzaki, R., Takeuchi, N., … Mori, H. (2018). Bipolar dispersal of red-snow algae. *Nature Communications*, **9**(1), 3094.

Takeuchi, N. (2001). The altitudinal distribution of snow algae on an Alaska glacier (Gulkana Glacier in the Alaska Range). *Hydrological Processes*, **15**(18), 3447–3459.

Takeuchi, N. (2013). Seasonal and altitudinal variations in snow algal communities on an Alaskan glacier (Gulkana glacier in the Alaska range). *Environmental Research Letters*, **8**(3), 035002.

Takeuchi, N., Dial, R., Kohshima, S., Segawa, T., & Uetake, J. (2006). Spatial distribution and abundance of red snow algae on the Harding Icefield, Alaska derived from a satellite image. *Geophysical Research Letters*, **33**(21), L21502.

U.S. Geological Survey Benchmark Glacier Program, Christopher J. Mcneil, Louis Sass, … Katherine E Bollen. (2024, December 11). Glacier-Wide Mass Balance and Compiled Data Inputs: USGS Benchmark Glaciers [Csv,zip], U.S. Geological Survey. doi:10.5066/F7HD7SRF

Wang, C., Mitsuya, Y., Gharizadeh, B., Ronaghi, M., & Shafer, R. W. (2007). Characterization of mutation spectra with ultra-deep pyrosequencing: Application to HIV-1 drug resistance. *Genome Research*, **17**(8), 1195–1201.

Yallop, M. L., Anesio, A. M., Perkins, R. G., … Roberts, N. W. (2012). Photophysiology and albedo-changing potential of the ice algal community on the surface of the Greenland ice sheet. *The ISME Journal*, **6**(12), 2302–2313.